Inactivation of *Escherichia coli* and somatic coliphage ΦX174 by oxidation of electrochemically produced Fe^{2+}

Bruno Bicudo [a,*], Gertjan Medema [a,b,c], Doris van Halem [a]

[a] *Faculty of Civil Engineering and Geosciences, Water Management Department, TU Delft, the Netherlands*
[b] *KWR Water Research Institute, the Netherlands*
[c] *Michigan State University, MI, USA*

ARTICLE INFO

ABSTRACT

Electrochemical ferrous iron (Fe^{2+}) wastewater treatment is gaining momentum for treating municipal wastewater due to its decreasing costs, environmental friendliness and capacity for removal of a wide range of contaminants. Disinfection by iron electrocoagulation (Fe-EC) has been occasionally reported in full scale industrial applications, yet controversy remains regarding its underlying elimination mechanisms and kinetics. In this study, it was demonstrated that substantial inactivation can be achieved for *Escherichia coli* WR1 (5 $\log_{10}$) and somatic coliphage ΦX174 (2–3 $\log_{10}$). Electrochemically produced Fe^{2+} yielded similar inactivation as chemical Fe^{2+}. Reactive oxygen species (ROS)-quenching experiments with TEMPOL confirmed that *E. coli* inactivation was related to the production of Fenton-like intermediates during Fe^{2+} oxidation. The observed *E. coli* disinfection kinetics could be mathematically related to Fe-EC current intensity using a Chick-Watson-like expression, in which the amperage is surrogate for the disinfectant's concentration. We hereby show that it is possible to mathematically predict disinfection based on applied Fe dosage and dosage speed. Phage ΦX174 inactivation could not be described in a similar way because at higher Fe dosages (>20 mg/l), little additional inactivation was observed. Also, ROS-quencher TEMPOL did not completely inhibit phage ΦX174 removal, suggesting that additional pathways are relevant for its elimination.

1. Introduction

Globally, agriculture is the largest water consumer worldwide. However, 3.2 billion people currently inhabit agricultural areas prone to shortages or severe scarcity [38]. The use of treated municipal wastewater is a common practice, particularly throughout Asia where over 200 million farmers make use of raw or treated wastewater for the irrigation of over 2000 km^2 of cropland [31–33]. In these cases, wastewater reuse can reduce the pressure on freshwater resources, particularly in water-stressed regions in which there can be extreme seasonal fluctuations in agricultural water availability. However, no matter how attractive municipal wastewater reclamation appears, it is still a potential source of a wide range of enteric pathogens. These include bacteria, viruses, protozoa and helminths, as well as the emerging concern of antimicrobial resistant bacteria, listed as a global health threat by WHO [9]. Hence, the reuse of municipal effluents

demands careful handling of the health risks associated with it. These risks will depend on the concentration of pathogens in the treated effluent, how the treated effluent will be used and the associated exposure routes and susceptibility of the users after exposure. Therefore, the level of treatment (pathogen inactivation) for reclamation purposes depends on the particular reuse application and the likelihood and frequency of user exposure.

In this study, we evaluated the disinfection[1] capacity of the electrochemical process called iron electrocoagulation (Fe-EC), targeting its use as a municipal water reclamation technology and with a special focus on its kinetics. Fe-EC is a process which releases Fe^{2+} ions into a water stream in order to induce coagulation, as opposed to conventional Fe chemical coagulation (CC), which is usually performed by dosing $FeCl_3$ or other Fe^{3+} salts. Fe-EC produces the metallic coagulant on site by the electrochemical dissolution of Fe (or steel) plates. Fe-EC has been applied as a treatment for effluents from a wide variety of industries,

---

[1] Disinfection is the process of water treatment to eliminate (pathogenic) microorganisms. Elimination mechanisms are inactivation of the microorganism or physical removal of the microorganism from the water matrix.

such as paper and pulp, petrochemical, textile, dairy, slaughterhouses, manure, metal-plating, and others ([7,10,28,46]). However, its use for municipal wastewater applications has been marginal and mainly confined to academic research [1,16,24,25,44].

Disinfection by Fe-EC has been occasionally reported in full scale industrial applications, yet its underlying inactivation mechanisms are still not clearly understood. In general terms, three major microbe removal/inactivation mechanisms have been proposed for Fe-EC, namely, (a) sorption or entrapment of microbes to the flocculation products with subsequent removal by sedimentation [3,12], (b) inactivation due to the induced electric field between the plates [8,29] and (c) chemical inactivation due to reactive oxygen species (ROS) [5,8,12,24,37] or due to the in-situ formation of disinfectants and disinfectant by-products [24,29].

Dixon & Stockwell [5] define ROS as a general term that includes several partially reduced molecules containing oxygen, such as superoxide ($^\bullet O_2^-$), peroxide (H_2O_2) and hydroxyl radicals ($^\bullet OH$). They are an integral part in the (semi)Fenton chemistry that takes place when Fe-EC is conducted under aerobic conditions, which comprises the aerobic oxidation pathway of Fe^{2+} into Fe^{3+} and the cascade of intermediate species formed in the process (Fig. 1). Most of these species, in particular the radicals, have an extremely short half-life in the range of 10^{-6} - 10^{-9} s, for which their production and degradation can be considered instantaneous [34]. In general terms, disinfection by ROS occurs due to oxidative damage to DNA/RNA, enzymes, proteins, cell membrane constituents (and subsequent rupture), viral capsids, phospholipid envelopes, or via the interruption of the respiratory pathway [4,20,41]. ROS disinfection capacity varies greatly among the different ROS species; while superoxide and hydrogen peroxide are considered the weakest ROS, compounds as hydroxyl radicals are considered the most potent.

Hence, during Fe-EC and CC there may be different pathways for inactivation or removal of (pathogenic) micro-organisms at play. However, to utilize Fe coagulation as a disinfection method, it is critical to differentiate between these pathways, as they require different operational conditions. The objective of this study was therefore to isolate the contribution of inactivation by ROS formed during Fe^{2+} oxidation from other removal pathways, such as floc sorption and entrapment, as this differentiation is generally lacking in electrocoagulation literature. The contribution of ROS-mediated inactivation was therefore assessed for both a bacterial and a viral enteric indicator organism, namely *Escherichia coli* WR1 and somatic coliphage ΦX174, respectively. For this purpose, a series of experiments with both chemical and electrochemical dosing of Fe^{2+} were conducted, either in presence or absence of the Fenton inhibitor TEMPOL [14]. In this study, a differentiation was made between continuous and single spike dosage, as it is hypothesized that continuous generation of ROS might be beneficial for the

disinfection capacity of the Fe-EC system. In addition, the dosage rate was assessed to develop a ROS-inactivation kinetics model for Fe-EC.

2. Materials and methods

2.1. Laboratory setup and experimental design

Experiments were conducted using Fe-EC and/or CC as sources of Fe (Fig. 2). All experiments were performed in 2 l cylindrical glass beakers mounted on identical LABNICO L23 magnetic stirrers and fitted with PTFE coated bars for stirring purposes. During all experiments, air was supplied continuously using an OASE OxyMax200 air pump, and dissolved oxygen (DO) levels were monitored continuously in order to maintain saturation in the test water.

Depending on the experiment, chemical dosing was performed either by spiking the dosage (weighing and directly dosing Fe salts into the reaction beaker), or by continuously adding dosing solutions using a Watson Marlow 120 U peristaltic pump. $FeCl_2$ and $FeCl_3$ reagent grade salts were supplied by Sigma-Aldrich (Germany). The Fe-EC setup included a 30 V - 3 A TENMA 72–10,500 bench DC power supply, connected with crocodile clip cables to two S235 steel plates (maximum percentages: 0.14% carbon, 0.10% silicium, 0.80% manganese, 0.025% phosphorous, 0.015% sulphur, 0.010% nitrogen, 0.20% copper and 0.080% aluminum). Dimensions of the steel plates were 6 cm × 4 cm, of which 4 cm × 4 cm were submerged (2 cm remained above the test water to connect the clip cables). The plates were polished with coarse and fine sand paper before each use and mounted to the end of a plastic tube with carved parallel slots ensuring the plates remained parallel and spaced approximately 1 cm as described elsewhere [1,2,12,26,29].

During each individual experiment, only two process-control parameters were adjusted, namely electrical current (amperage) and electrolysis time. These parameter combinations were selected beforehand for each experiment in order to produce a dose of 50 mgFe/l under different speeds, namely 5.0, 2.5, and 1.0 mgFe/l/min, as oxidation kinetics are relevant for this research. The maximum Fe dosage rate (5.0 mgFe/l/min) was selected based on the capacity of the power supply not to reach/exceed its maximum voltage (30 V). Since experiments were conducted at room temperature, the need to minimize 'spontaneous' inactivation of *E. coli* limited the duration of the experiments, which in turn defined the lower Fe dosage rate (1.0 mgFe/l/min). An intermediate Fe dosage speed (2.5 mgFe/l/min) was added as a third dataset.

Four groups of experiments were performed in order to determine the role of oxidizing Fe^{2+} in ROS-mediated disinfection (Fig. 3) and the kinetics involved. For all experiments, synthetic water containing a buffer solution and indicator microbes was prepared (described in Section 2.2). The contribution of ROS-mediated disinfection was assessed in two ways, namely, 1) comparing inactivation by Fe^{2+} or Fe^{3+} and 2)
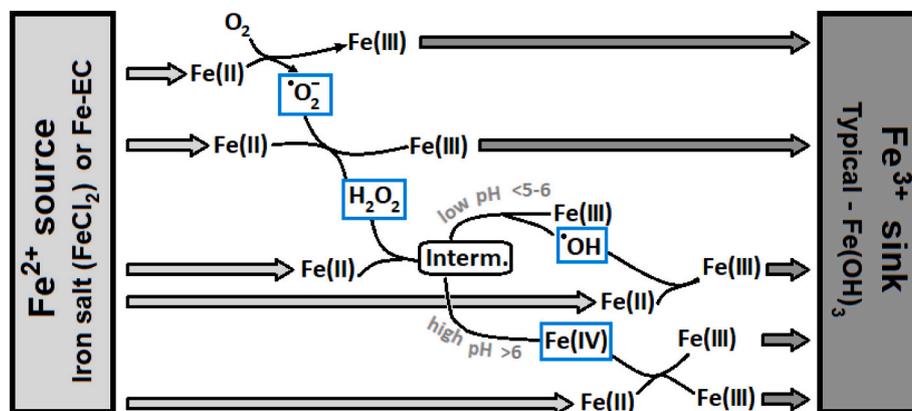

Fig. 1. Proposed pathways of aerobic Fe^{2+} oxidation, indicating the production of ROS: superoxide radical ($^\bullet O_2^-$), hydrogen peroxide (H_2O_2), hydroxyl radical ($^\bullet OH$) and high valent oxoiron (FeIV). Adapted from [15,18,39].
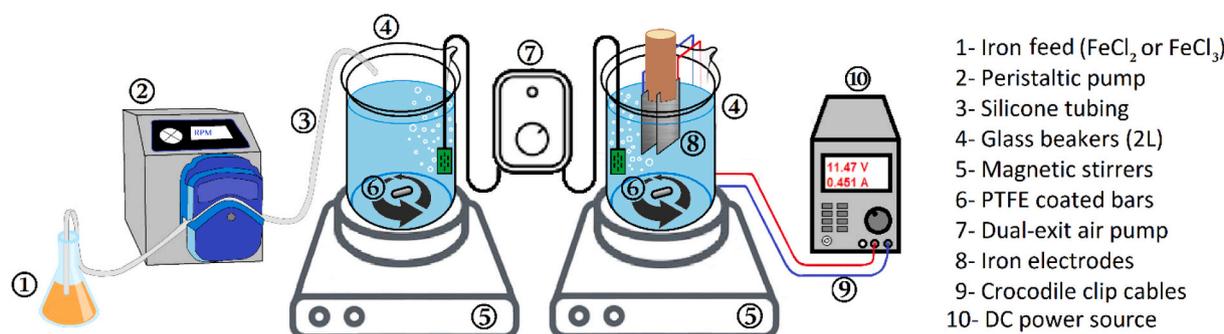
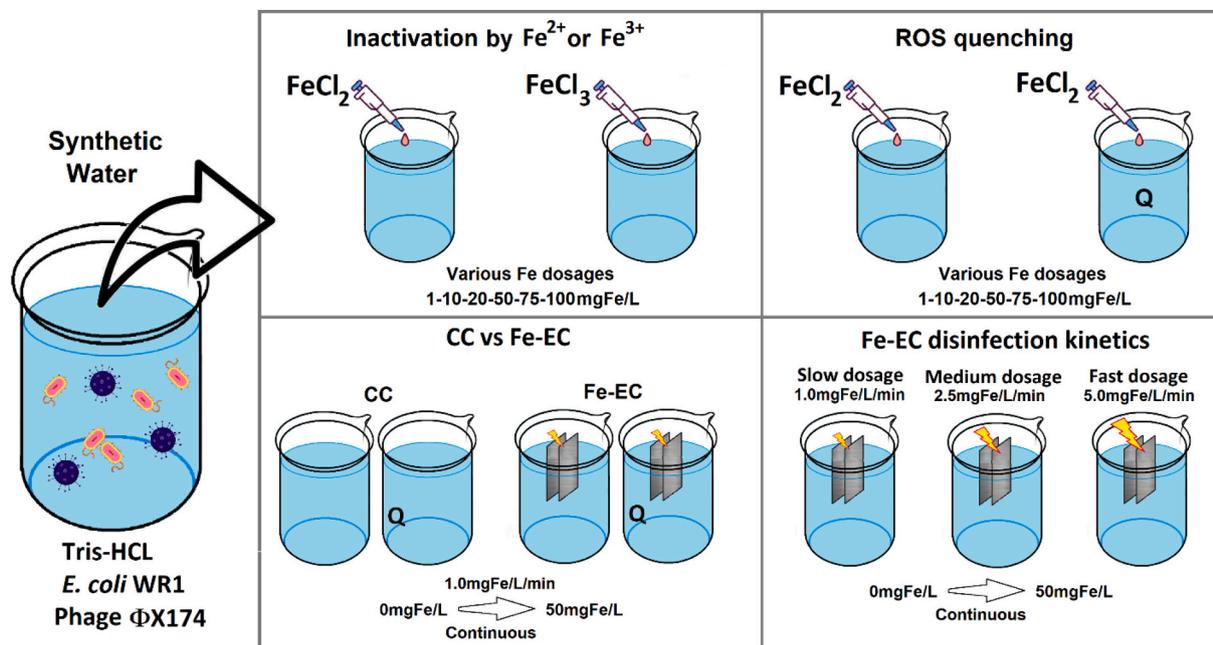**Fig. 2.** Fe dosage bench scale setup, with chemical dosage (left) and electrochemical dosage (right).

Fig. 3. Schematic description of the four Fe disinfection experiments. Letter "Q" indicates the beaker was dosed with an ROS-Quencher. Pipette represents single-event chemical dosage, while the arrow represents continuous dosage either by CC (FeCl$_2$ solution dosed with peristaltic pump) or Fe-EC (Fe dosed electrochemically under a constant current).

ROS quenching while dosing Fe^{2+} (FeCl$_2$) (see 2.4). To determine whether the source of Fe had any impact on ROS-mediated disinfection, a third group of experiments compared microbial inactivation using CC or Fe-EC as the Fe^{2+} source (including ROS quenching for each case). Lastly, Fe-EC disinfection kinetics were studied by operating the system at different dosage rates. Additional information can be found in S.I. Table 1.

For all experiments, the stirring speed was set to 200 rpm, which induced intense mixing and turbulence, and prevented the formation of macroscopic flocs. Samples were collected immediately after the Fe dosing was stopped (while the stirring was still on), in order to avoid any sedimentation. Collected samples were used immediately for microbiological and physical/chemical characterization.

2.2. Synthetic water matrix

For all experiments, the synthetic water matrix was either 0.02 M or 0.04 M tris-HCl buffer ((HOCH$_2$)$_3$CNH$_2$) (S.I. Table 1), selected by its capacity to buffer at a pH of approximately 7.5–7.7 (similar to that of municipal secondary effluents), its absence of Fe or ROS scavengers (such as PO$_4^{3-}$, CO$_3^{2-}$, Ca^{2+}), and its moderate conductivity (avoiding the addition of electrolytes for Fe-EC).

2.3. Microbial spike preparation

Two non-pathogenic organisms were used to spike the synthetic effluents, namely *E. coli* WR1 (NCTC 13167) and somatic coliphage ΦX174 (ATCC 13706-B1), a bacterial and viral indicator respectively, as previously used in [2]. *E. coli* WR1 frozen stock was thawed and grown in TYGB broth (Tryptone Yeast Extract Glucose Broth) for 3 h at 37 °C to concentrations of ≈1 × 10^8 cfu/ml, then centrifuged at 10.000 rpm during 10 min. The obtained pellet was re-suspended in PBS pH 7.2 to a concentration of ≈1 × 10^9 cfu/ml, stored at 4 °C and used within 24 h. Phage ΦX174 was propagated following the ISO 10705-2:2000 method (Water quality — Detection and enumeration of bacteriophages — Part 2: Enumeration of somatic coliphages), to concentrations of approximately ≈1 × 10^9 pfu/ml. *E. coli* WR1 and phage ΦX174 were dosed into the test liquid to initial concentrations of ≈1 × 10^5 cfu/ml and ≈1 × 10^4 pfu/ml, respectively.

2.4. TEMPOL as quencher for Fe^{2+}-mediated ROS

In order to inhibit the disinfection by ROS produced following the aerobic oxidation of Fe^{2+}, 4-hydroxy-2,2,6,6-tetramethylpiperidin-1-oxyl (also known as 4-Hydroxy-TEMPO, or TEMPOL) was selected as

ROS quencher. TEMPOL is the most studied of the nitroxides, mainly due to its low molecular weight and high cell permeability [43]. Its most remarkable properties include the superoxide catalysis, the catalytic destruction of H_2O_2 by catalase-like reactions and the hindering of toxic hydroxyl radical production.

The reaction between TEMPOL and Fe^{2+} cations was described by [27]:

$$RR'NO^\bullet + Fe^{2+} \Rightarrow RR'NOH + Fe^{3+} \qquad (1)$$

In this reaction, the nitroxide (indicated by the reducible functional group $-NO^\bullet$) reacts on a 1:1 M ratio with Fe^{2+}, to produce the oxidized oxoammonium ($-NOH$) and Fe^{3+}. In this way, nitroxides accept the electrons from reduced Fe complexes, therefore outcompeting oxygen, and thus preventing the production of oxygenated radicals. This equimolar reaction between Fe^{2+} and TEMPOL was instrumental during ROS-quenching experiments later described in this publication. During these experiments, reagent grade TEMPOL (Sigma-Aldrich –Germany), was weighed, added directly and diluted into the synthetic water before any addition of Fe.

2.5. Analytical methods

E. coli screening and quantification was performed by membrane filtration according to APHA-Standard Methods for the Examination of Water and Wastewater, 23rd Edition. Samples were filtered in 0.45 μm cellulose acetate membrane filters, and placed on Chromocult® Coliform Agar (Merck) selective media (in which *E. coli* WR1 yields distinct purple colonies), and incubated at 37 °C for 24 h. Screening of somatic coliphages was performed by pour plate technique following ISO 10705-2:2000. Total Fe was measured with Spectroquant®Iron Cell Test (1–50 mgFe/l) using a Spectroquant®NOVA60 (Merck, Germany) photometer, while Fe^{2+} was measured with Hach LCK 320 Fe test kits (0.2–6 mgFe/l). Hydrogen peroxide measurements were conducted following the Ghormley triiodide method [6] with filtered samples (0.45 μm) using a Genesys 10S UV–Vis (Thermo Scientific) at 350 nm wavelength. All samples analyzed for H_2O_2 were processed within 60 s of extraction. For Fe-EC experiments, free chlorine tests were conducted in filtered samples using the DPD method (Spectroquant- Supelco) in order to rule out the production of Cl_2 compounds that could account for unwanted disinfection.

2.6. Data analysis

A reduction in the concentration of the microorganisms is expressed as log removal values since this term is widely used, but here referred to as either *removal* or *inactivation* based on the involved elimination

mechanism. Comparison between data series of somatic coliphage ΦX174 or *E. coli* concentrations in synthetic effluents under different conditions was performed using Spearman's Rank-Order Correlation, which calculates rank correlation coefficient (R_s) and *p*-value. R_s determines the strength of the correlation between two datasets ($R_s > 0.9$ indicates very strong correlation). The p-value determines the likelihood of two data series to be co-relatable by mere chance (p-value <0.05 shows a strong correlation beyond chance between data sets). Spearman was preferred over Pearson's correlation due to the monotonic behavior of most plots to be correlated (Section 3).

3. Results

3.1. Inactivation by Fe^{2+} or Fe^{3+}

Experiments comparing *E. coli* WR1 and somatic coliphage ΦX174 inactivation by varying dosages of either Fe^{2+} or Fe^{3+} are depicted in Fig. 4. No significant difference in terms of floc characteristics were observed after 1 h of continuous stirring, for samples dosed with either $FeCl_2$ or $FeCl_3$ (S.I. Fig. 4). For both selected microbial indicators, inactivation using $FeCl_3$ (Fe^{3+}) was negligible across all assayed dosages, yet the response towards $FeCl_2$ (Fe^{2+}) was considerably different. *E. coli* inactivation increased with increasing Fe^{2+} dosage, with an approximate 0.05 $\log_{10}$ per mg Fe/l dosed. At the maximum dosage of 100 mg Fe/l, *E. coli* inactivation approached 5 $\log_{10}$. The inactivation of ΦX174 showed a biphasic pattern; up to 10–20 mg Fe^{2+}/l inactivation was more rapid (close to 1.5 $\log_{10}$), which was similar to *E. coli*, while at higher Fe^{2+} concentrations, inactivation levelled off, reaching approximately 2.5 $\log_{10}$ at 100 mg Fe/l. All retrieved samples dosed with $FeCl_2$ showed full Fe^{2+} oxidation after 1 h of stirring (Fe^{2+} below Limit of Detection - LOD), though given the relatively high pH and DO, it is likely that this condition had been achieved within minutes. It may be concluded that under intense mixing (to prevent sedimentation) and aerobic conditions, dosage of Fe^{2+} demonstrated to have considerable inactivation properties that were not observed for Fe^{3+} under identical conditions. This indicates that the oxidation of Fe^{2+} itself, and potentially the production of intermediate ROS, plays a critical role in Fe-based disinfection.

3.2. ROS quenching

To investigate the contribution of ROS to *E. coli* and ΦX174 inactivation during Fe^{2+} oxidation, Fe^{2+} was dosed chemically with and without the presence of an equimolar amount of the ROS-quencher TEMPOL. TEMPOL counteracted the bactericidal properties of oxidizing Fe^{2+} for *E. coli*, with under 1 $\log_{10}$ inactivation at all dosages
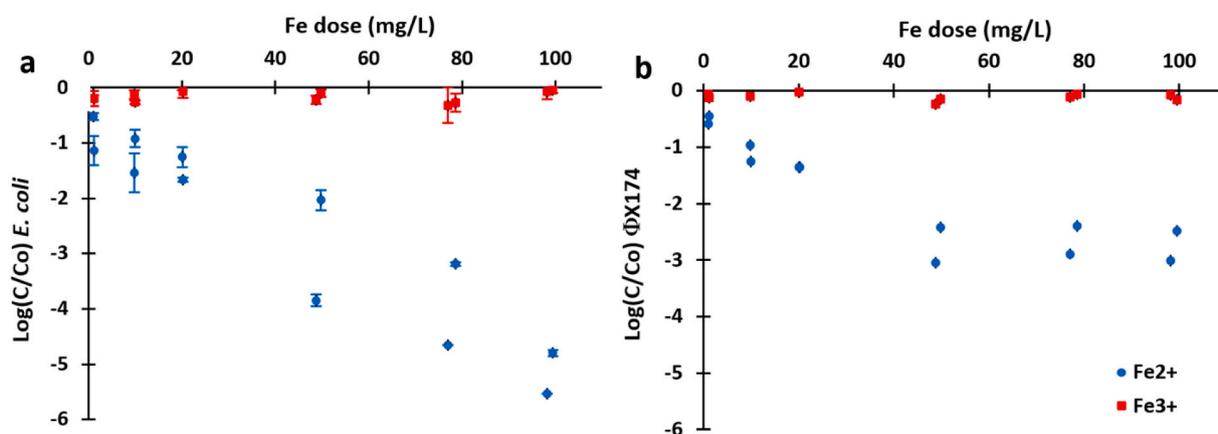

Fig. 4. Inactivation of (a) *E. coli* WR1 and (b) somatic coliphage ΦX174 during dosing 0–100 mg/l of either Fe^{2+} or Fe^{3+}. Error bars represent standard deviation. All experiments were performed in duplicate, and all microbial determinations were executed in triplicate.

(S.I. Fig. 1). According to Eq. (1), the interaction between TEMPOL and Fe^{2+} should lead to oxidation of the latter into Fe^{3+} without O_2 acting an as electron acceptor, avoiding the formation of the superoxide radical, and thus halting the ROS cascade. All samples (with and without TEMPOL) showed full Fe oxidation after 1 h of stirring (Fe^{2+} below LOD). Inactivation of *E. coli* and phage ΦX174 under a dose of 50 mgFe/l is displayed in Fig. 5. The complete dosage series is presented in S.I. Fig. 1. For both indicators, beakers in which only TEMPOL was dosed showed almost identical microbial concentrations as the blank (negligible inactivation), confirming that the quencher itself did not exhibit inactivation properties. *E. coli* inactivation reached approximately 3 log_{10} when the reaction was not quenched, dropping to <0.5 log_{10} with TEMPOL added. These results indicate that the observed inactivation during Fe^{2+} oxidation was related to the formation of reactive intermediates, and that this inactivation pathway could be almost completely suppressed by the addition of the Fenton inhibitor TEMPOL. This also indicates that the primary elimination process was inactivation rather than entrapment in flocs. Phage ΦX174 demonstrated a similar inactivation as *E. coli* under the presence of Fe^{2+} (≈ 2.8 log_{10}) without TEMPOL, while inactivation was still significant after the addition of TEMPOL (1.5 log_{10}). The observation that ΦX174 disinfection in the presence of TEMPOL is not fully suppressed suggests the contribution of an elimination mechanism other than ROS, such as entrapment in flocs. No production of Cl_2-based compounds (<0.01 mg/l total Cl_2) was detected during these or any of the experiments described in this publication, hence this inactivation mechanism was ruled out.

3.3. CC versus Fe-EC

To determine the impact of the source of Fe^{2+} in inactivation, experiments using an identical and constant Fe supply rate (1.0 mgFe/l/min) were conducted, either by CC or Fe-EC. For *E. coli* WR1, almost identical inactivation was obtained whether the Fe source was either chemical ($FeCl_2$) or electrochemical (Fig. 6a). This indicated that the source of Fe^{2+} was irrelevant for inactivation as long as the produced Fe^{2+} dosage was similar (Spearman's Rank Correlation test between averaged data sets determined $R_s \approx 1$ with a *p*-value of 0.001). For both CC and Fe-EC, the Fe was dosed in a constant manner instead of in a single spike, as instant dosing is not possible with Fe-EC. When comparing Fe^{2+} continuous dosing (Fig. 6 a,c) against instant dosing

Fig. 5. Log Removal of *E. coli* WR1 (left) and somatic coliphage ΦX174 (right) under Fe^{2+}, Fe^{2+}+ TEMPOL, and only TEMPOL (equimolar concentrations of 0.9 mM ≈ 50 mgFe/l and/or 154.5 mgTEMPOL/l). Error bars represent standard deviation. All experiments were performed in duplicate and all microbial determinations were executed in triplicate.

(Figs. 4 and 5) for inactivation of *E. coli*, it is apparent that for constant dosing the same maximum inactivation is achieved after dosing only half the Fe dose (50 mgFe/l) than for the single spike experiments (100 mgFe/l). For phage ΦX174, experiments with non-quenched Fe^{2+} also produced similar inactivation results whether the Fe source was chemical ($FeCl_2$) or electrochemical, as depicted in Fig. 6c. This indicated that the source of Fe^{2+} is also irrelevant for phage ΦX174 inactivation as long as the produced Fe dosage is similar (Spearman $R_s = 0.97$; *p*-value = 0.001). Regarding the performance of continuous Fe dosing compared to a single spike (Figs. 4 and 5), 50 mgFe/l continuous dosage yielded similar inactivation of ΦX174 as a single spike dose (≈ 2 log_{10} inactivation). For experiments involving quenched Fe^{2+} dosage (with added TEMPOL), inactivation datasets coming from the *E. coli* experiments with chemical and electrochemical sources still show a statistically strong correlation (Spearman $R_s = 0.86$, p-value = 0.05), but inactivation is in either case almost completely mitigated under the presence of TEMPOL (Fig. 6b). Inactivation was ≈ 1 log_{10} at the maximum Fe dosage (50 mgFe/l). Data for ΦX174 experiments involving quenched Fe^{2+} dosage (Fig. 6d), on chemical versus electrochemical sources again showed a statistically strong correlation (Spearman $R_s = 0.93$, p-value = 0.02). However, as opposed to the strong reduction of the inactivation rate observed for *E. coli* (Fig. 6b versus 6a), addition of TEMPOL yielded only a small reduction of the inactivation rate for either of the Fe sources (Fig. 6d versus 6c).

Altogether, these results conclusively show that irrespective of the type of assay (quenched/non-quenched) or the type of microbial indicator, there is no statistical difference between inactivation induced by Fe^{2+} coming from either CC or Fe-EC. This implies that during Fe-EC, the contribution of electrolysis-specific inactivation pathways (due to electric fields or to Cl_2 formation) was negligible.

3.4. Fe-EC inactivation kinetics

In order to investigate Fe-EC inactivation kinetics, experiments were conducted with three different dosing rates, namely 5.0, 2.5 and 1.0 mgFe/l/min (fast, medium and slow dosage, respectively). For each of these settings, the Fe supply was stopped once the cumulative dosage reached 50 mgFe/l in order to produce the same end concentration.

For *E. coli* WR1, the faster the Fe dosage, the higher the inactivation rate. Interestingly, inactivation stopped abruptly once the electric charge was interrupted, which means that the inactivation produced during the Fe-EC stage offered no residual effect once the current ceased (S.I. Fig. 2). This implies that disinfectants produced during the supply of Fe^{2+} were extremely short lived. The plot Ln(C/Co) versus electrolysis time (Fig. 7a) shows a good correlation between the averaged datasets and linear trendlines, with the slope being the inactivation rate, in which the ratios between the inactivation rates (5.2/3.0/1.0) are similar to the ratios of the current intensity and of Fe production speed (5.0/2.5/1.0). When plotted against the Fe dosage (Fig. 7b), there is an overlap between the Ln(C/Co) plots, indicating that inactivation is directly proportional to the dosed Fe for all dosage speeds.

For phage ΦX174, results showed different inactivation kinetics than *E. coli*: the inactivation rate (the slope in Fig. 7c) appeared numerically comparable for all experiments. This means that the inactivation rate progressed similarly irrespective of dosing speed as long as the electric current was being applied, yet was independent of the magnitude of such current (instead of proportional as for *E. coli*). Since each configuration delivered different amounts of Fe per unit time, shorter Fe dosage times (faster dosage speeds) yielded less total inactivation than slower dosages, as depicted in Fig. 7d. For 50 mgFe/l, the slow dosage speed (1.0 mgFe/l/min) produced ≈ 4.7 Ln inactivation (1.8 log_{10}), whereas the fast dosage speed (5.0 mgFe/l/min) reached only 1.2 Ln (0.7 log_{10}). The averaged Ln(C/Co) diagrams for each different charge speed condition show sufficient linearity as to assume a linear regression to provide an adequate fit, even though the R^2 values were somewhat lower than those obtained for *E. coli*. For all cases, the decrease in the
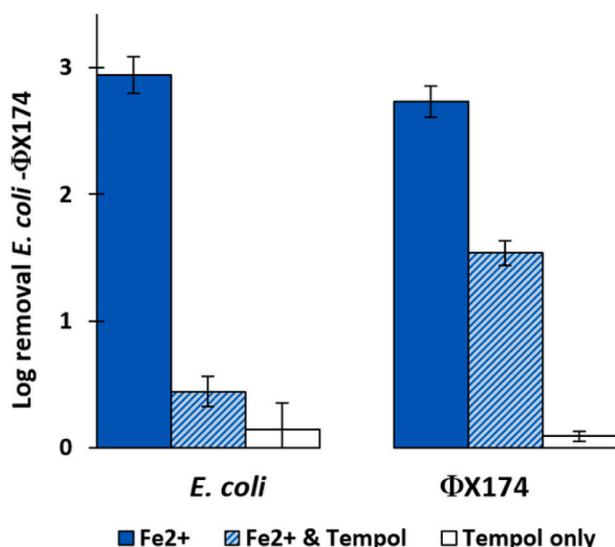
Fig. 6. Inactivation of *E. coli* under CC and Fe-EC without TEMPOL (a) and with TEMPOL (b), and inactivation of phage ΦX174 under CC and Fe-EC without TEMPOL (c) and with TEMPOL (d). Error bars represent standard deviation. All experiments were performed in duplicate, and all microbial determinations were executed in triplicate.
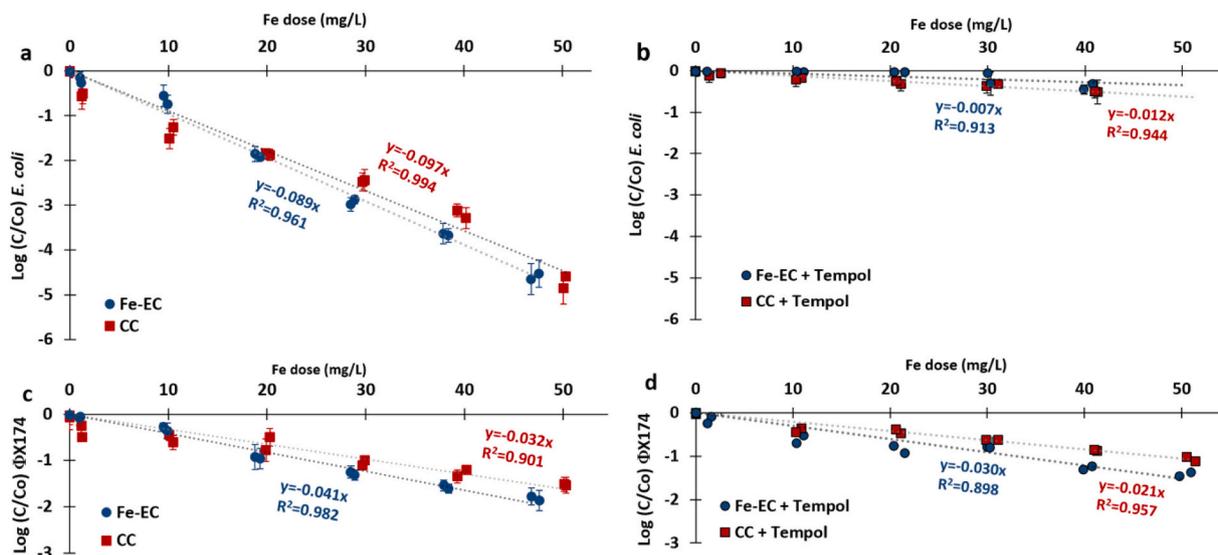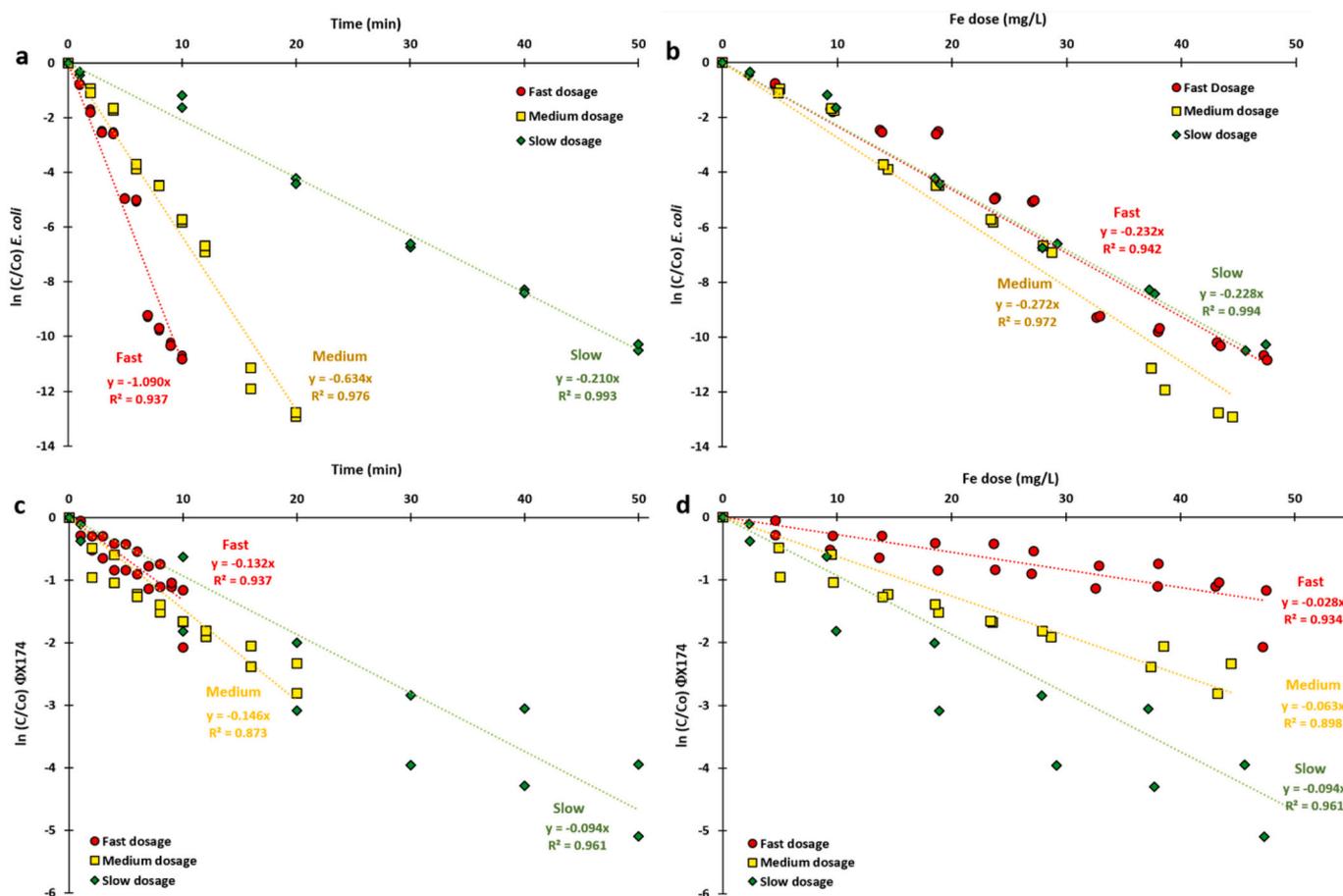

Fig. 7. Ln(C/Co) plot for *E. coli* WR1 concentration during the application of fast, medium and slow electrochemical Fe dosage as a function of (a) time and (b) dosed Fe, and Ln(C/Co) plot for phage ΦX174 concentration during the application of fast, medium and slow electrochemical Fe dosage as a function of (c) time and (d) dosed Fe. All experiments were performed in duplicate, and all microbial determinations were executed in triplicate.

concentration of phage ΦX174 ceased abruptly once the electric current supply was interrupted (as was the case with *E. coli*), once again suggesting that Fe-EC produced no residual disinfection, and that the disinfectants produced were extremely short lived (S.I. Fig. 3).

3.5. Fe speciation and H_2O_2 measurements

During the Fe-EC inactivation kinetics experiments, screening of Fe^{2+} and Fe^{3+} was performed to verify that the conversion of Fe^{2+} into Fe^{3+} was a steady-state process. H_2O_2 screening was performed simultaneously, to confirm the onset of the ROS cascade. Fe screening (Fig. 8) showed, for all cases, a very stable and relatively low Fe^{2+} concentration being established and measured during electrolysis, simultaneous with a stable Fe^{3+} production. Since Fe is electrochemically dosed as Fe^{2+} [22], and Fe^{3+} is produced at a steady rate, this means that Fe^{2+} is readily converted to Fe^{3+}. This was expected due to relatively high pH (7.4–7.7) and dissolved oxygen close to saturation (>7.5 mgO_2/l). Once the current was interrupted, an abrupt drop in the Fe^{2+} concentration was observed, readily stabilizing at ≈ 1 mgFe/l for the remainder of the screening. It is important to note that in all cases inactivation only occurred during the time in which Fe^{2+} was being steadily supplied (and steadily oxidized), and halted abruptly once Fe^{2+} stopped being supplied (hence stopped being oxidized). For all experiments, Faradaic efficiency of the Fe-EC was determined ≈ 95–96%.

Based on the measured Fe^{2+} plateau, pH and dissolved oxygen concentrations during Fe-EC, theoretical Fe^{2+} oxidation rates (or Fe^{3+} production) were calculated following the methodology proposed by Stumm & Lee [36] expressed in Eq. (2). Calculations are detailed in S.I. Table 3.

$$-\frac{d\left[Fe^{2+}\right]}{dt} = k.\left[Fe^{2+}\right].p_{O_2}.[OH^-]^2 \qquad (2)$$

where:

k is the kinetic constant $1.5 \pm 0.5 \times 10^{13}$ $L^2mol^{-2}atm^{-1}min^{-1}$
$[Fe^{2+}]$ is the molar concentration of the Fe present in the Fe^{2+} form
p_{O2} is the partial pressure of oxygen (atm)
$[OH^-]$ is the molarity of the OH^- ion

Theoretical versus observed oxidation rates are displayed in Table 1:
These theoretical Fe^{2+} oxidation values are numerically very similar to the measured production rate of Fe^{3+} in each case (4.69, 2.36 and 0.93 mgFe/l/min, respectively), confirming that the obtained Fe^{2+} concentrations and oxidation rates during the application of electric current corresponded to that of a (pseudo) steady-state.

Samples for H_2O_2 measurement were collected every 1, 2 or 5 min for fast, medium and slow dosage respectively, and processed according to the Ghormley triiodide method after 0.45 µm filtration, as turbid samples yield very high false readings. The maximum observed value for H_2O_2 occurred during fast dosage, reaching ≈ 1.07 mg/l (53.7 µM) at $t = 8$ min, while for the medium and slow dosage experiments the maximum was approximately at 0.25 ± 0.05 mg/l (13.9 µM), as depicted in Fig. 9. During slow dosage, a sudden drop of H_2O_2 concentration from 0.27 mg/l to below detection was observed once the current was

Table 1
Theoretical versus observed average Fe^{2+} oxidation rate, as a function of pH and D.O for each dosage condition.

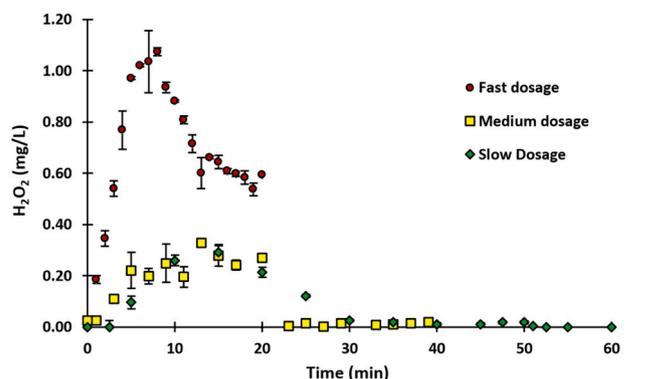|	Dosage		
	Fast	Medium	Slow
pH	7.75	7.70	7.70
D. O. (mg/l)	7.6	7.8	9.1
Fe^{2+} plateau (mg/l)	4.8	2.9	1.6
d[Fe^{2+}]/dt (mg/l/min) - Stum & Lee	4.78	2.29	1.29
d[Fe^{2+}]/dt (mg/l/min) - measured	4.69	2.36	0.93

Fig. 9. Average H_2O_2 production profiles during fast, medium and slow Fe dosage. All experiments were performed twice. Error bars represent standard deviation.

disconnected, suggesting that the H_2O_2 conversion rate into intermediates (Fig. 1) is much faster than the experimental measurement time. This could imply that the actual H_2O_2 value inside of the beaker at the moment of sample extraction could be larger than the value actually measured 60s later, this being an important limitation of the H_2O_2 measurement method. It is unlikely however, that H_2O_2 was responsible for disinfection since the required concentrations and exposure time for inactivation are orders of magnitude larger than the ones observed [21]. However, the production of H_2O_2 is a necessary intermediate step in the ROS-cascade, mediating in the production of hydroxyl radicals and/or ferryl ions (the main disinfecting species related to Fe-ROS), as depicted in Fig. 1.

4. Discussion

4.1. Inactivation of E. coli and phage ΦX174 by Fe^{2+} oxidation: role of ROS

Electrochemically produced Fe^{2+} yielded significant inactivation in
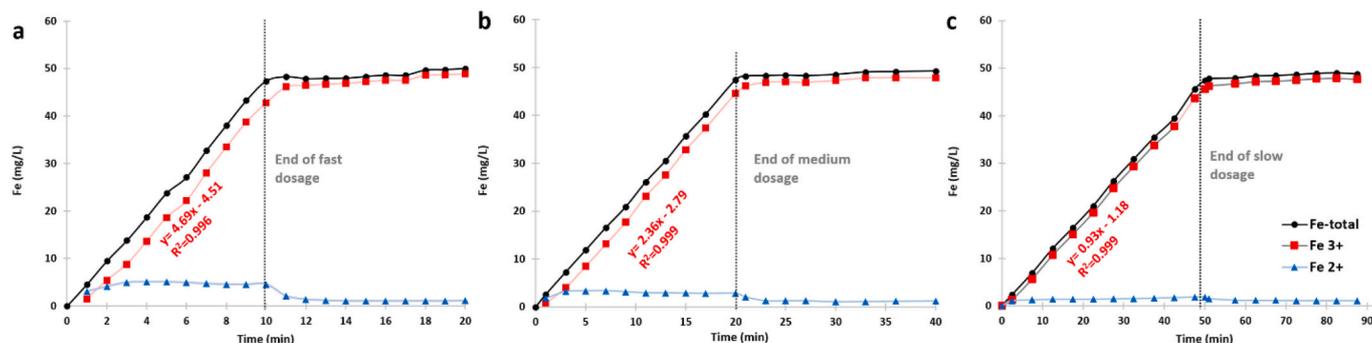

Fig. 8. Fe profiles (Total Fe, Fe^{2+} and Fe^{3+}) during (a) fast dosage (b) medium dosage and (c) slow dosage. The best fitting linear equation and R^2 for the Fe^{3+} series (during Fe supply) is indicated in each case, together with the timestamp in which Fe supply is stopped. All experiments were performed in duplicate.

synthetic secondary effluent at pH 7.5–7.7 at room temperature (20 °C) under intensive mixing and aeration, reaching 5 $\log_{10}$ for *E. coli* at 100 mg/l Fe^{2+}. It was suggested that the oxidation of Fe^{2+} promotes the formation of bactericidal ROS species [1], while Fe^{3+} is unable to do so given its already oxidized state [17,40]. This hypothesis was tested by the introduction of the Fenton inhibitor TEMPOL in order to verify if the anoxic oxidation of Fe^{2+} into Fe^{3+} would lose its disinfection capacities, as the quencher would theoretically accept the produced electron (instead of the O_2) preventing the ROS formation [23,30,35]. Indeed, the addition of TEMPOL resulted in the almost complete inhibition of the inactivation of *E. coli*, underlining the value of dosing Fe in its reduced state.

For phage ΦX174, electrochemically produced Fe^{2+} also resulted in inactivation, but the net result was lower than for *E.coli* (2 versus 5 $\log_{10}$ at 100 mg/l Fe^{2+}). A biphasic inactivation pattern was observed for ΦX174, with faster inactivation up to 10–20 mg/l Fe^{2+} and slower inactivation between 20 and 100 mg/l Fe^{2+}. For the phage, the quencher did reduce inactivation, but to a considerably smaller extent than for *E. coli*, pointing towards an additional removal pathway other than ROS. Such an alternative pathway was proposed by [18], who determined

$$Ln\left(\frac{N}{N_0}\right) = -K.Fe_{dosed} \tag{4}$$

where:

K = first order rate constant
N = concentration of *E. coli*
N_0 = starting concentration of *E. coli*
Fe_{dosed} = cumulative dosage of Fe

The data series obtained for fast, medium and slow dosage had very similar slopes, varying from 0.23 to 0.27 $mgFe^{-1}$ with an average slope of 0.24 $L.mgFe^{-1}$, being therefore selected as the value K. The Fe dose can in turn be expressed as the product of Fe dosing rate (d[Fe]/dt) and electrolysis time (Eq. (5)), hence:

$$Ln\left(\frac{N}{N_0}\right) = -0.24.\frac{d[Fe]}{dt}.t \tag{5}$$

Based on Faraday's equation (S.I. Eq. (1)), the term d[Fe]/dt can be obtained as follows:

$$m_{Fe} = \frac{I.t.M}{n.F}\eta \xrightarrow{/Vol} [Fe] = \frac{I.t.\ 55.85 g.mol^{-1}}{V.2.96485.3\ C\ mol^{-1}}\eta \xrightarrow{/dt} \frac{d[Fe]}{dt} = \frac{I.\ 2.90x10^{-4}g.C^{-1}}{V}\eta \tag{6}$$

that un-oxidized Fe^{2+} achieved measurable MS2 phage inactivation, although it proved to be weak under aerobic conditions and relatively low Fe^{2+} concentrations, as in our experiments. [45] found that MS2 bacteriophages adsorb to the Fe oxyhydroxide flocs due to their negative surface charge, and [19] demonstrated that virus entrapment and inactivation take place during Fe-EC. [12], and [13] proposed that phage inactivation was promoted by longer exposure time of the viruses to the ROS, which aligns with our findings for different Fe-EC dosing rates. However, in our experiments, TEMPOL did not fully shield phage ΦX174 from inactivation (Fig. 6c and d) since a decrease in plaque counts was observed even when ROS were believed to be suppressed. This points to either a separate simultaneous inactivation process or to marginal ROS production due to O_2 competition for Fe^{2+} that could not be sufficiently quenched by TEMPOL.

4.2. Fe-EC inactivation kinetics of phage ΦX174 and E. coli

Inactivation of phage ΦX174 increased with apparent linearity with the Fe-EC dosage time. The variation of the value k (0.094 to 0.140 min^{-1}) is relatively small considering the 500% variation of the current intensity, meaning that the inactivation rate is largely irresponsive to it. With this, we conclude that exposure time to oxidizing Fe^{2+} is the main driver in phage inactivation:

$$Ln\left(\frac{N}{N_0}\right) = -k_n.t \tag{3}$$

where:

-k_n is a first order rate constant (ranges from 0.094 to 0.140 min^{-1}, derived from Fig. 7c).
-t is the electrolysis time (min)

Phage ΦX174 inactivation was found to be dependent of time, but not of the dosed Fe. The Ln(C/Co) plot for *E. coli* WR1, however, clearly showed linearity towards the Fe dose. Therefore, the expression linking *E. coli* WR1 inactivation to the dosed Fe can be written as follows:

where:

m_{Fe} = mass of released Fe (g)
I = Intensity of the electric current (A)
t = time of electrolysis (s)
M = Molar mass of the sacrificial anode metal (Fe = 55.85 g/mol)
n = valence of the released metal ion (for Fe n = 2)
F = Faraday's constant (96,485.3C/mol)
[Fe] = Concentration of Fe (g/L)
V = Sample volume (L)
η = Faradaic efficiency (0.95–0.96 during these experiments)

Converting concentrations and time into mgFe and min respectively in Eq. (6), and substituting in Eq. (5), a simple expression can be obtained for the Ln(N/No), resulting in Eq. (7):

$$Ln\left(\frac{N}{N_0}\right) = -\frac{I.t}{V}.\eta.4.08\frac{L}{A.min} \tag{7}$$

Since both the assay volume and Faradaic efficiency are assumed to be constant, the obtained expression has the same structure as the well-known Chick-Watson equation [42], namely:

$$Ln\left(\frac{N}{N_0}\right) = -K_{cw}.C.t \tag{8}$$

In this expression K_{cw} is a specific inactivation constant, t is the exposure time to the disinfectant, and C is the concentration of such disinfectant. In our particular case, the current intensity behaves as a pseudo-disinfectant, not because the electric current is producing inactivation, but because the release of the disinfectant's precursor (Fe^{2+}) is directly proportional to the current intensity (I).

Applying a logarithmic base change:

$$Log_{10}\left(\frac{N}{N_0}\right) = -\frac{I.t}{V}x\,\eta\,x\,1.77\frac{L}{A.min} \tag{9}$$

This expression shows that for a given time [min] and sample volume [L], the logarithmic removal value of *E. coli* WR1 is directly proportional

to the current intensity [A]. The adjustment coefficient (1.77 L.A^{-1}. min^{-1}) is then a function of the environmental conditions (pH, DO, temperature, etc.). To the best of our knowledge, this expression is the first to link disinfection with electric current during Fe-EC.

4.3. Chemical or electrochemical Fe^{2+}

When comparing inactivation results of CC with Fe-EC, it may be concluded that the origin of the Fe^{2+} source did not play a significant role in disinfection. It could be argued, however, that the final hydrolysis products and the floc formation process are different, even though both experiments were conducted under identical test conditions (pH, temperature, mixing intensity, DO). The differences between chemical and electrochemical floc forming processes were extensively studied by Harif et al. [11], who concluded that the coagulation/flocculation mechanisms using either coagulation method are similar yet not identical. It was found that electrocoagulation produced more fragile and porous flocs, which are easily compacted and restructured. The high shear conditions in our experiments prevented the formation of macroscopic floc-like structures (7–11 μm range; S.I. Table 2), producing what could best be described as fine dust-sized particles. The flocs, however, did not play a significant role in the elimination of *E. coli,* as the addition of TEMPOL almost completely stopped inactivation. For ΦX174, inactivation was less prominent and also less affected by TEMPOL, suggesting that another elimination process (e.g., entrapment in flocs) was also important. This could differ between CC and Fe-EC, however, the potential contribution of differences in Fe(OH)$_3$ floc structure on microbial entrapment was beyond the scope of this study. What is apparent is that experiments using Fe^{3+} did not produce observable differences with the no-treatment blank for either microbial indicator, pointing out that Fe^{3+} or its particulates offered no measurable disinfection properties (inactivation nor floc entrapment) under these high shear conditions.

5. Conclusions

In this study it was demonstrated that *E. coli* WR1 and somatic coliphage ΦX174 are inactivated during Fe^{2+} oxidation, irrespective of dosing Fe chemically or electro-chemically. In control experiments with Fe^{3+}, no inactivation was observed for either microbe. ROS-quenching experiments with TEMPOL confirmed that *E. coli* inactivation (5 log$_{10}$) is related to the production of Fenton-like intermediates (ROS) during Fe^{2+} oxidation. The observed *E. coli* inactivation kinetics could be mathematically related to the Fe^{2+} oxidation rate, which under aerobic conditions is also directly proportional to the Fe-EC current's intensity. The inactivation process then follows a Chick-Watson-like expression, in which the amperage behaves as a surrogate for the disinfectant's concentration. Phage ΦX174 removal/inactivation (2–3 log$_{10}$) could not be described in the same way, as at higher Fe dosages (>10 mg/l) removal efficiency dropped rapidly. Also, ROS-quencher TEMPOL did not completely inhibit phage ΦX174 inactivation, suggesting that additional pathways are relevant for virus removal.

Declaration of competing interest

The authors declare that they have no known competing financial interests or personal relationships that could have appeared to influence the work reported in this paper.

Acknowledgments

Appendix A. Supplementary data

Supplementary data to this article can be found online at https://doi. org/10.1016/j.jwpe.2022.102683.

References

[1] E. Anfruns-Estrada, C. Bruguera-Casamada, H. Salvadó, E. Brillas, I. Sirés, R. M. Araujo, Inactivation of microbiota from urban wastewater by single and sequential electrocoagulation and electro-Fenton treatments, Water Res. 126 (2017) 450–459, https://doi.org/10.1016/j.watres.2017.09.056.

[2] B. Bicudo, D. van Halem, S.A. Trikannad, G. Ferrero, G. Medema, Low voltage iron electrocoagulation as a tertiary treatment of municipal wastewater: removal of enteric pathogen indicators and antibiotic-resistant bacteria, Water Res. 188 (2021), https://doi.org/10.1016/j.watres.2020.116500.

[3] C. Delaire, C.M. van Genuchten, S.E. Amrose, A.J. Gadgil, Bacteria attenuation by iron electrocoagulation governed by interactions between bacterial phosphate groups and Fe(III) precipitates, Water Res. 103 (2016) 74–82, https://doi.org/ 10.1016/j.watres.2016.07.020.

[4] E.A.S. Dimapilis, C.S. Hsu, R.M.O. Mendoza, M.C. Lu, Zinc oxide nanoparticles for water disinfection, Sustain. Environ. Res 28 (2) (2018) 47–56, https://doi.org/ 10.1016/j.serj.2017.10.001.

[5] S.J. Dixon, B.R. Stockwell, The role of iron and reactive oxygen species in cell death, Nat. Chem. Biol. 10 (1) (2014) 9–17, https://doi.org/10.1038/ nchembio.1416.

[6] J.E. Frew, P. Jones, G. Scholes, Spectrophotometric determination of hydrogen peroxide and organic hydroperoxides at low concentrations in aqueous solution, Anal. Chim. Acta 155 (C) (1983) 139–150, https://doi.org/10.1016/S0003-2670 (00)85587-7.

[7] S. Garcia-Segura, M.M.S.G. Eiband, J.V. de Melo, C.A. Martínez-Huitle, Electrocoagulation and advanced electrocoagulation processes: A general review about the fundamentals, emerging applications and its association with other technologies, in: Journal of Electroanalytical Chemistry, vol. 801, Elsevier B.V., 2017, pp. 267–299, https://doi.org/10.1016/j.jelechem.2017.07.047.

[8] D. Ghernaout, B. Ghernaout, From chemical disinfection to electrodisinfection: the obligatory itinerary? Desalin. Water Treat. 16 (1–3) (2010) 156–175, https://doi. org/10.5004/dwt.2010.1085.

[9] Global Antimicrobial Resistance and Use Surveillance System (GLASS) Report 2021, 2021. https://www.who.int/health-topics/antimicrobial-resistance% 0AISBN.

[10] J.N. Hakizimana, B. Gourich, M. Chafi, Y. Stiriba, C. Vial, P. Drogui, J. Naja, Electrocoagulation process in water treatment: a review of electrocoagulation modeling approaches, in: Desalination, vol. 404, Elsevier B.V., 2017, pp. 1–21, https://doi.org/10.1016/j.desal.2016.10.011.

[11] T. Harif, M. Khai, A. Adin, Electrocoagulation versus chemical coagulation: coagulation/flocculation mechanisms and resulting floc characteristics, Water Res. 46 (10) (2012) 3177–3188, https://doi.org/10.1016/j.watres.2012.03.034.

[12] J. Heffron, B. McDermid, E. Maher, P.J. McNamara, B.K. Mayer, Mechanisms of virus mitigation and suitability of bacteriophages as surrogates in drinking water treatment by iron electrocoagulation, Water Res. 163 (2019), https://doi.org/ 10.1016/j.watres.2019.114877.

[13] J. Heffron, D.R. Ryan, B.K. Mayer, Sequential electrocoagulation-electrooxidation for virus mitigation in drinking water, Water Res. 160 (2019) 435–444, https:// doi.org/10.1016/j.watres.2019.05.078.

[14] Y. Hu, J. Wang, H. Sun, S. Wang, X. Liao, J. Wang, T. An, Roles of extracellular polymeric substances in the bactericidal effect of nanoscale zero-valent iron: trade-offs between physical disruption and oxidative damage, Environ. Sci. Nano 6 (7) (2019) 2061–2073, https://doi.org/10.1039/c9en00354a.

[15] S.J. Hug, O. Leupin, Iron-catalyzed oxidation of Arsenic(III) by oxygen and by hydrogen peroxide: pH-dependent formation of oxidants in the Fenton reaction, Environ. Sci. Technol. 37 (12) (2003) 2734–2742, https://doi.org/10.1021/ es026208x.

[16] M. Ikematsu, K. Kaneda, M. Iseki, H. Matsuura, M. Yasuda, Electrolytic treatment of human urine to remove nitrogen and phosphorus, Chem. Lett. 35 (6) (2006) 576–577, https://doi.org/10.1246/cl.2006.576.

[17] J. Jeong, J.Y. Kim, J. Yoon, The role of reactive oxygen species in the electrochemical inactivation of microorganisms, Environ. Sci. Technol. 40 (19) (2006) 6117–6122, https://doi.org/10.1021/es0604313.

[18] J.Y. Kim, C. Lee, D.C. Love, D.L. Sedlak, J. Yoon, K.L. Nelson, Inactivation of MS2 coliphage by ferrous ion and zero-valent iron nanoparticles, Environ. Sci. Technol. 45 (16) (2011) 6978–6984, https://doi.org/10.1021/es201345y.

[19] K. Kim, N. Jothikumar, A. Sen, J.L. Murphy, S. Chellam, Removal and inactivation of an enveloped virus surrogate by iron conventional coagulation and electrocoagulation, Environ. Sci. Technol. 55 (4) (2021) 2674–2683, https://doi. org/10.1021/acs.est.0c07697.

[20] K. Kim, J. Narayanan, A. Sen, S. Chellam, Virus Removal and Inactivation Mechanisms during Iron Electrocoagulation: Capsid and Genome Damages and Electro- Fenton Reactions., 2021, https://doi.org/10.1021/acs.est.0c04438.

[21] M.D. Labas, C.S. Zalazar, R.J. Brandi, A.E. Cassano, Reaction kinetics of bacteria disinfection employing hydrogen peroxide, Biochem. Eng. J. 38 (1) (2008) 78–87, https://doi.org/10.1016/j.bej.2007.06.008.

[22] D. Lakshmanan, D.A. Clifford, G. Samanta, Ferrous and ferric ion generation during iron electrocoagulation, Environ. Sci. Technol. 43 (10) (2009) 3853–3859, https://doi.org/10.1021/es8036669.

[23] M. Lewandowski, K. Gwozdzinski, Nitroxides as antioxidants and anticancer drugs, Int. J. Mol. Sci. 18 (11) (2017), https://doi.org/10.3390/ijms18112490.

[24] J. Llanos, S. Cotillas, P. Cañizares, M.A. Rodrigo, Effect of bipolar electrode material on the reclamation of urban wastewater by an integrated electrodisinfection/electrocoagulation process, Water Res. 53 (2014) 329–338, https://doi.org/10.1016/j.watres.2014.01.041.

[25] B. Malinovic, D. Bjelić, T. Đuričić, The phosphate removal efficiency electrocoagulation wastewater using iron and aluminum electrodes, 2016. https://www.researchgate.net/publication/313238550.

[26] B. Merzouk, B. Gourich, A. Sekki, K. Madani, M. Chibane, Removal turbidity and separation of heavy metals using electrocoagulation-electroflotation technique. A case study, J. Hazard. Mater. 164 (1) (2009) 215–222, https://doi.org/10.1016/j.jhazmat.2008.07.144.

[27] J.B. Mitchell, A. Samuni, M.C. Krishna, W.G. DeGraff, M.S. Ahn, U. Samuni, A. Russo, Biologically active metal-independent superoxide dismutase mimics, Biochemistry 29 (11) (1990) 2802–2807, https://doi.org/10.1021/bi00463a024.

[28] D.T. Moussa, M.H. El-Naas, M. Nasser, M.J. Al-Marri, A comprehensive review of electrocoagulation for water treatment: Potentials and challenges, J. Environ. Manag. 186 (2017) 24–41, https://doi.org/10.1016/j.jenvman.2016.10.032.

[29] A.C. Ndjomgoue-Yossa, C.P. Nanseu-Njiki, I.M. Kengne, E. Ngameni, Effect of electrode material and supporting electrolyte on the treatment of water containing Escherichia coli by electrocoagulation, Int. J. Environ. Sci. Technol. 12 (6) (2015) 2103–2110, https://doi.org/10.1007/s13762-014-0609-9.

[30] M. Nyui, Ikuo Nakanishi, T.O. Kazunori Anzai, K. M., Reactivity of redox sensitive paramagnetic nitroxyl contrast agents with reactive oxygen species, J. Clin. Biochem. Nutr. 62 (2) (2018) 179–186, https://doi.org/10.3164/jcbn.17.

[31] M. Qadir, B.R. Sharma, A. Bruggeman, R. Choukr-Allah, F. Karajeh, Non-conventional water resources and opportunities for water augmentation to achieve food security in water scarce countries, Agric. Water Manag. (2007), https://doi.org/10.1016/j.agwat.2006.03.018.

[32] M. Qadir, D. Wichelns, L. Raschid-Sally, P.G. McCornick, P. Drechsel, A. Bahri, P. S. Minhas, The challenges of wastewater irrigation in developing countries, Agric. Water Manag. 97 (4) (2010) 561–568, https://doi.org/10.1016/j.agwat.2008.11.004.

[33] L. Raschid-sally, P. Jayakody, Drivers and characteristics of wastewater agriculture in developing countries: results from a global assessment, in: International Water Management Institute (Issue IWMI Research Report 127), 2008, https://doi.org/10.3910/2009.127.

[34] C.P. Rubio, J.J. Cerón, Spectrophotometric assays for evaluation of Reactive Oxygen Species (ROS) in serum: general concepts and applications in dogs and humans, BMC Vet. Res. 17 (1) (2021) 1–14, https://doi.org/10.1186/s12917-021-02924-8.

[35] B.P. Soule, F. Hyodo, K.ichiro Matsumoto, N.L. Simone, J.A. Cook, M.C. Krishna, J. B. Mitchell, The chemistry and biology of nitroxide compounds, Free Radic. Biol. Med. 42 (11) (2007) 1632–1650, https://doi.org/10.1016/j.freeradbiomed.2007.02.030.

[36] W. Stumm, G.F. Lee, Oxygenation of Ferrous Iron, 1961. www.gfredlee.com.

[37] C.T. Tanneru, S. Chellam, Mechanisms of virus control during iron electrocoagulation - microfiltration of surface water, Water Res. 46 (7) (2012) 2111–2120, https://doi.org/10.1016/j.watres.2012.01.032.

[38] UN-Water, Summary Progress Update 2021 : SDG 6 — water and sanitation for all. 58. https://www.unwater.org/new-data-on-global-progress-towards-ensuring-water-and-sanitation-for-all-by-2030/, 2021.

[39] C.M. Van Genuchten, J. Peña, Mn(II) oxidation in Fenton and Fenton type systems: identification of reaction efficiency and reaction products, Environ. Sci. Technol. 51 (5) (2017) 2982–2991, https://doi.org/10.1021/acs.est.6b05584.

[40] F. Vatansever, W.C.M.A. de Melo, P. Avci, D. Vecchio, M. Sadasivam, A. Gupta, R. Chandran, M. Karimi, N.A. Parizotto, R. Yin, G.P. Tegos, M.R. Hamblin, Antimicrobial strategies centered around reactive oxygen species - bactericidal antibiotics, photodynamic therapy, and beyond, FEMS Microbiol. Rev. 37 (6) (2013) 955–989, https://doi.org/10.1111/1574-6976.12026.

[41] M.J. Villaseñor, Á. Ríos, Nanomaterials for water cleaning and desalination, energy production, disinfection, agriculture and green chemistry, Environ. Chem. Lett. 16 (1) (2018) 11–34, https://doi.org/10.1007/s10311-017-0656-9.

[42] H.E. Watson, A note on the variation of the rate of disinfection with change in the concentration of the disinfectant, Epidemiol. Infect. 8 (4) (1908) 536–542, https://doi.org/10.1017/S0022172400015928.

[43] C.S. Wilcox, A. Pearlman, Chemistry and antihypertensive effects of tempol and other nitroxides, Pharmacol. Rev. 60 (4) (2008) 418–469, https://doi.org/10.1124/pr.108.000240.

[44] L. Zaleschi, C. Sáez, P. Cañizares, I. Cretescu, M.A. Rodrigo, Electrochemical coagulation of treated wastewaters for reuse, Desalin. Water Treat. 51 (16–18) (2013) 3381–3388, https://doi.org/10.1080/19443994.2012.749192.

[45] B. Zhu, D.A. Clifford, S. Chellam, Virus removal by iron coagulation-microfiltration, Water Res. 39 (20) (2005) 5153–5161, https://doi.org/10.1016/j.watres.2005.09.035.

[46] H. Bergmann, Electrochemical disinfection – State of the art and tendencies, Curr. Opin. Electrochem. 28 (2021), 100694, https://doi.org/10.1016/j.coelec.2021.100694.